

1 Physical and stoichiometric controls on stream respiration in a 2 headwater stream 3

4 Jancoba Dorley¹, Joel Singley^{2,3}, Tim Covino^{4,5}, Kamini Singha⁶, Michael Gooseff^{7,8}, [David Van](#)
5 [Horn](#)⁹, Ricardo González-Pinzón¹

6 *Correspondence to:* Ricardo González-Pinzón (gonzaric@unm.edu)

7 ¹Civil, Construction and Environmental Engineering, University of New Mexico, Albuquerque, NM USA

8 ²Environmental Studies Program, University of Colorado, Boulder, CO USA

9 ³Biology, Marine Biology, and Environmental Science, Roger Williams University, Bristol, RI USA

10 ⁴Ecosystem Science and Sustainability, Colorado State University, Fort Collins, CO USA

11 ⁵Department of Land Resources and Environmental Sciences, Montana State University, Bozeman, MT USA

12 ⁶Geology and Geological Engineering, Hydrologic Science and Engineering Program, Colorado School of Mines,
13 Golden, CO USA

14 ⁷Civil, Environmental and Architectural Engineering, University of Colorado, Boulder, CO USA

15 ⁸Institute of Arctic and Alpine Research, University of Colorado, Boulder, CO USA

16 ⁹[Department of Biology, University of New Mexico, Albuquerque, NM USA](#)

17
18 **Abstract.** Many studies in ecohydrology focusing on hydrologic transport argue that longer residence times across a
19 stream ecosystem should consistently result in higher biological uptake of carbon, nutrients, and oxygen. This
20 consideration does not incorporate the potential for biologically mediated reactions to be limited by stoichiometric
21 imbalances. Based on the relevance and co-dependences between hydrologic exchange, stoichiometry, and
22 biological uptake, and acknowledging the limited amount of field studies available to determine their net effects on
23 the retention and export of resources, we quantified how microbial respiration is controlled by the interactions and
24 supply of essential nutrients ~~needed~~ (C, N, P) in a headwater stream in Colorado, USA. For this, we conducted two
25 rounds of nutrient experiments, each consisting of four sets of continuous injections of Cl⁻ as a conservative tracer,
26 resazurin as a proxy for aerobic respiration, and one of the following nutrient treatments: a) N, b) N+C, c) N+P, and
27 d) C+N+P. Nutrient treatments were considered as known system modifications to alter metabolism, and statistical
28 tests helped identify the relationships between hydrologic transport and respiration metrics. We found that as
29 discharge changed significantly between rounds and across stoichiometric treatments, a) transient storage mainly
30 occurred in ~~side-pools along-lateral to~~ the main channel and was proportional to discharge, and b) microbial
31 respiration remained similar between rounds and across stoichiometric treatments. ~~Our results contradict the notion~~
32 ~~that hydrologic transport alone is a dominant control on biogeochemical processing and suggest that complex~~
33 ~~interactions between hydrology, resource supply, and biological community function are responsible for driving in-~~
34 ~~stream respiration. Together, our results indicate that residence time alone could be a weak predictor of stream~~
35 ~~respiration due to the relevance of local and dynamic variations in stoichiometric conditions.~~
36
37

38 1 Introduction

39 High biochemical processing rates in streams and rivers occur at locations and times where the dynamic
40 interconnections among hydrologic exchange, residence time, nutrient supply, and microbial biomass combine to
41 form optimum conditions for metabolic activity (i.e., the transformation of nutrients, carbon, and oxygen or another
42 electron acceptor into energy and biomass). The exchange of water between the main channel and transient storage
43 zones, where most microbes exist, is the primary mechanism supplying carbon, nutrients, and oxygen to
44 metabolically active zones (Gooseff et al. 2004; Covino et al. 2010b, 2011; Knapp et al. 2017; Gootman et al.
45 2020). The extent of water exchange controls the residence time of solutes (Drummond et al., 2012; Gomez et al.,
46 2012; Patil et al., 2013), their chemical signatures (Covino and McGlynn 2007), as well as the microbial
47 composition and their metabolic functioning (Blume et al. 2002; Navel et al. 2011; Li et al. 2020). Exchange
48 patterns are influenced by geomorphologic conditions (Kasahara and Wondzell 2003; Cardenas et al. 2004; Gooseff
49 et al. 2005; Emanuelson et al. 2022), hydrologic conditions (i.e., discharge and surrounding water table
50 configuration) (Gooseff et al. 2005; Wondzell 2006; Ward et al. 2013; Ward and Packman 2019), and ~~even~~-biofilm
51 growth (Battin et al. 2003; Wen and Li 2018). The spatiotemporal variability in exchange processes and resource
52 availability (e.g., seasonal variations in nutrient loads) create heterogeneous hydrologic and biogeochemical
53 gradients across space and time, within which ecosystem metabolism occurs (Mulholland et al., 1985; Mulholland &
54 Hill, 1997).

55 To date, studies with a focus on hydrologic transport argue that longer residence times across a stream
56 ecosystem should consistently result in higher biological demand for carbon, nutrients, and oxygen (Valett et al.
57 1996; Gooseff et al. 2005; Wondzell 2006; Gomez et al. 2012; Zarnetske et al. 2012; Ward et al. 2013; Li et al.
58 2021), not fully incorporating the potential for biologically mediated reactions to be limited by stoichiometric
59 imbalances. Ecological stoichiometry is the notion that biota balances the consumption of nutrients with energy
60 requirements. Redfield (1934) noted that marine phytoplankton generally contained a ratio of C:N:P of 106:16:1 in
61 their biomass, and these ratios are similar to those available in their environment. This “Redfield ratio” suggests that
62 an ecosystem requires an optimal ~~distribution-ratio~~ of available nutrients to flourish and has been used as a guide for
63 many other environmental stoichiometry studies. In a study of streams across eight biomes, Dodds et al.
64 (2004) noted that N ~~retention-consumption~~ depends in part on the C:N ratio of organic matter in streams and
65 suggested that shifts in these state ratios likely influence N retention.

66 The net effect of supply and demand of resources can be explored with the non-dimensional Damköhler
67 number, Da (Harvey et al. 2013; Pinay et al. 2015; Krause et al. 2017; Ocampo et al. 2020), which quantifies the
68 ratio of transport (i.e., supply) to biological uptake (i.e., demand) timescales along flow paths (Oldham et al. 2013;
69 Liu et al. 2022). Similar to any other non-dimensional number, Da offers simplicity and objectivity for inter-site and
70 intra-site comparisons. Da has been used to provide insight into the factors limiting the supply and demand of
71 resources (Harvey et al. 2005), as values of $Da \sim 1$ define a balance between transport and uptake time scales, which
72 theoretically result in maximal resource retention. Accordingly, where or when $Da \ll 1$, i.e., the uptake timescale is
73 much greater than the transport timescale, uptake is suboptimal, and it is referred to as reaction limited because even
74 though resources became available through hydrologic exchange, they were not fully taken up (i.e., assimilated).

75 Conversely, where or when $Da \gg 1$, i.e., the transport timescale is much greater than the uptake timescale, resources
76 become scarce or transport-limited, and biologically inactive subregions start to develop (González-Pinzón and
77 Haggerty 2013; Harvey et al. 2013; Gootman et al. 2020). While Da captures essential components of the potential
78 interactions between the supply and demand of ecologically relevant resources, it does not explicitly capture the role
79 of stoichiometric limitations on the supply (i.e., C:N:P ratios in water fluxes) and demand (C:N:P biomass
80 composition and needs) of resources (Tromboni et al. 2018). This is ~~mainly~~ because Da numbers are estimated from
81 solute-specific mass balances, which inform transport and reaction timescales for one resource at a time (e.g., only
82 N), in isolation of other stoichiometrically relevant resources that can become limiting factors (e.g., C and P).

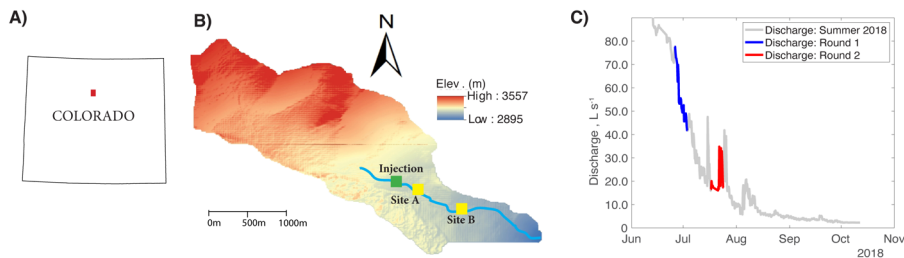
83 Based on the relevance and co-dependences between hydrologic exchange, stoichiometry, and biological
84 uptake, and the limited amount of field studies available to determine their net effects on the retention and export of
85 resources, we sought to quantify how metabolic activity is controlled by the interactions and supply of essential
86 nutrients (C, N, P). More specifically, we tested if variations in stoichiometric conditions can induce metabolic
87 limitations at which residence time alone becomes a weak predictor of stream respiration. We addressed the
88 following research question: *How is microbial respiration controlled by hydrologic exchange vs. stoichiometric*
89 *conditions (i.e., supply of C, N, and P)?* We hypothesized that aerobic respiration would be maximized when
90 nutrient supply and demand were nearly balanced for a given hydrologic condition. To test this, we conducted a
91 repeated set of stream tracer injections in Como Creek, a mountain stream in Colorado, USA, varying stream C
92 (acetate; sensu Baker et al., 1999), N (NaNO_3), and P (KH_2PO_4) concentrations to manipulate stoichiometry and
93 nutrient supply. We repeated experiments under different flow conditions to quantify the tradeoffs between supply
94 (transport and delivery of nutrients), and demand (microbial respiration). We tested for statistical relationships
95 between hydrologic transport metrics and respiration metrics using the resazurin-resorufin tracer system (González-
96 Pinzón et al., 2012; Knapp et al., 2018) and contextualized our findings within the framework of the Damköhler
97 number.

98 2 Methods

99 2.1 Site Description

100 Our research experiments were conducted in Como Creek, a forested pool and riffle stream in Colorado,
101 USA. Como Creek is a tributary to Boulder Creek, with land cover consisting of approximately 20% alpine
102 meadow-tundra and 80% conifer forest. The study reach drains a 5.4 km² catchment, with elevations ranging from
103 2895-3557 m and a mean average precipitation of 883 mm/y (Ries III et al. 2017; Emanuelson et al. 2022). Como
104 Creek has a snowmelt-driven hydrograph with stream discharges ranging from 1-98 L/s and features short-lived
105 increases in discharge during the monsoon season between July and August (Figure 1). The study reach is a multi-
106 thread channel with substrate ranging from small gravel to bedrock. Additionally, the channel has an average width-
107 to-depth ratio of 11.5, a sinuosity of 1.1, and an average longitudinal slope of 21% (Natural Resources Conservation
108 Service).

109



110
111 **Figure 1:** A) Location of Como Creek watershed in Colorado, B) detailed map of the watershed where Sites A and B are
112 50 and 350 m downstream from the injection location, and C) hydrograph and timing of experimental work; each round
113 of experiments consisted of four treatments featuring N, N+C, N+P, and C+N+P nutrient additions.
114

115 2.2 Stream tracer injection experiments

116 We conducted two rounds of experiments, each consisting of four sets of continuous injections (lasting ~ 4-
117 7 h) of Cl⁻ as a conservative tracer, resazurin (referred to as Raz hereafter) as a proxy for aerobic respiration, and one
118 of the following nutrient treatments: a) N, b) N+C, c) N+P, and d) C+N+P. In our study, the nutrient treatments are
119 treated as known system modifications (control variables) to alter metabolism. Also, we use the transformation of
120 Raz, which occurred at the same spatiotemporal scales of the nutrient additions, to calculate how changes in
121 stoichiometric conditions and discharge affect respiration. Briefly, the reactive tracer Raz (blue in color) is
122 irreversibly reduced to resorufin (Rru, red) under aerobic respiration, and the relationship between Raz
123 transformation and oxygen consumption is linear (González-Pinzón et al. 2012, 2014, 2016; Knapp et al. 2018;
124 Dallan et al. 2020).

125 Before each tracer injection, we used the Tracer Injection Planning Tool (TIPT) (González-Pinzón et al.
126 2022) to estimate the amount of ~~commercial~~ tracer mass needed to reach steady state conditions at the downstream
127 site and to estimate the duration of the tracer breakthrough curves. From our field sampling, ambient concentrations
128 of nitrate averaged 0.035 (±0.002) mg/L. We corroborated this value with a study by (Smith et al. 2003), who
129 generated estimates of background total nitrogen (TN) and total phosphorous (TP) yield and concentrations
130 throughout the stream-river network in 14 ecoregions of the conterminous US. That study found 75th % quartile TN=
131 0.21 (±0.05) mg/L and TP= 0.02 (±0.005), which indicates relatively low nutrient concentrations compared to
132 agricultural streams in the US Midwest featuring ambient concentrations of up to two orders of magnitude higher.
133 Based on estimated discharges and reach lengths, we targeted a maximum concentration of 2 mg/L for Cl, and 100
134 µg/L at the most downstream locations. The concentrations for nitrogen, phosphorus, and carbon were based on the
135 expected detection limit of phosphate (i.e., 0.1 mg/L) for common ion chromatographs. From that minimum
136 phosphate concentration expected, we scaled the masses of nitrogen and carbon using the 106C:16N:1P Redfield
137 ratio (Redfield, 1934). Table 1 shows the masses injected and the discharges observed during the studies. Note that
138 we allowed the stream to return to ambient concentrations for one day after each set of injections.

141

Table 1: Tracer injection data for each round of experiments at Como Creek.

Date	Treatment	Discharge (L/s)	Start time	End time	NaCl (g)	KNO ₃ (g)	KPO ₄ (g)	Sodium Acetate (g)	Raz (g)
Round 1									
6/26/18	N	74	11:30	17:00	32653	502	-	-	150
6/28/18	N+C	61	10:08	14:10	32680	500	-	2000	150
6/30/18	N+P	53	10:00	17:00	32680	500	400	N/A	150
7/2/18	C+N+P	49	9:59	14:00	32680	500	400	2000	150
Round 2									
7/17/18	N	20	10:30	14:35	10000	100	-	-	30
7/19/18	N+C	17	10:00	13:59	10000	100	-	400	30
7/21/18	N+P	17	10:00	14:06	10000	100	80	-	30
7/23/18	C+N+P	25	9:30	13:35	10000	100	80	400	30

142

143

144

145

146

147

148

149

150

151

152

153

154

155

156

157

158

159

We collected 20 mL aliquots in each tracer injection 50m and 350m downstream of the injection site (labeled Sites A and B, Figure 1) to generate tracer breakthrough curves (BTCs) for Raz. All samples were filtered immediately after being collected using a 0.7 μm GF/F filter (Sigma-Aldrich) and kept on dry ice during transport until they were frozen at -4°C for laboratory analysis for Raz concentrations. All analyses took place within a week after the end of each round of injections. At the laboratory, each sample was buffered to a pH of 8.5 (1:10 buffer-to-sample) following Knapp et al. (2018). The fluorescence signals were measured with a Cary Eclipse Fluorescence Spectrophotometer (Agilent Technologies) using excitation/emission wavelengths of 602/632 nm for Raz and 571/584 nm for Rru and converted to concentrations based on an 8-point calibration curve (R²=0.99).

We monitored specific conductivity (SC) and temperature using Campbell Scientific CS547A sensors connected to Campbell Scientific CR 1000 dataloggers, which recorded and stored those measurements every 10 minutes. From the grab samples, we measured chloride using a Dionex ICS-1000 Ion Chromatograph with AS23/AG23 analytical and guard columns. Cl data were augmented with background-corrected SC data to model conservative transport.

We monitored changes in stream stage every 10 minutes at the end of the study reach using pressure transducers (Campbell Scientific CS420) connected to a datalogger (Campbell Scientific CR 1000). We used established stage-discharge relationships specific for the study site, as provided by the site managers. The discharge values reported in Table 1 represent mean values observed during a given experiment.

160

2.2 Conservative transport modelling and metrics

161

162

163

164

We calibrated the conservative transport parameters of the transient storage model presented in Equations 1 and 2 using Cl⁻ and streamwater electrical conductivity data observed at Sites A and B. For this, we used the Matlab (The Mathworks Inc., Natick, Massachusetts) script from Knapp et al. (2018), which features a joint calibration of conservative and reactive solutes through a non-linear, least squares optimization routine.

165

$$\frac{\partial c}{\partial t} = -u \frac{\partial c}{\partial x} + D \frac{\partial^2 c}{\partial x^2} - \frac{A_s}{A} \frac{\partial c_{ts}}{\partial t} + q_{in} c - \lambda_{mc} c \quad (1)$$

166

$$\frac{\partial c_{ts}}{\partial t} = k(c - c_{ts}) - \lambda_{ts} c_{ts} \quad (2)$$

$$\frac{\partial c}{\partial t} = -u \frac{\partial c}{\partial x} + D \frac{\partial^2 c}{\partial x^2} - \frac{A_s}{A} \frac{\partial c_{ts}}{\partial t} + q_{in} c - \lambda_{mc} c \quad (1)$$

$$\frac{\partial c_{ts}}{\partial t} = k(c - c_{ts}) - \lambda_{ts} c_{ts} \quad (2)$$

167
168 where c [ML⁻³] and c_{ts} [ML⁻³] are the concentrations in the main channel and aggregate transient storage zone; x
169 [L] is the distance of the study reach; t [T] is time; u [LT⁻¹] and D [L²T⁻¹] are parameters representing advective
170 flow velocity and dispersion coefficient, respectively; q_{in} [T⁻¹] is a volumetric flux parameter accounting for lateral
171 inputs; k [T⁻¹] is the first-order mass transfer rate coefficient parameter between the main channel and the aggregate
172 transient storage zone; A_s/A [-] is the capacity ratio parameter representing the relative contribution of transient
173 storage-dominated to advection-dominated compartments in the stream, represented as areas along the reach; and
174 λ_{mc} and λ_{mets} [T⁻¹] are processing-rate coefficients in the main channel and transient storage zones (equaling zero
175 for a conservative tracer).

176 We completed the parameter estimation using the Differential Evolution Adaptive Metropolis (DREAM
177 [ZS]) algorithm (Andersson (Vrugt et al. 2009)). We jointly fit Cl- and Raz data in a first step of 100,000 model
178 generations. We assessed model convergence using Gelman and Rubin R statistics (Gelman and Rubin 1992). The
179 goodness of fit between measured and simulated BTCs was quantified through the calculation of the residual sum of
180 squares, (nRSS) (-), normalized by the squared theoretical peak tracer concentrations of each tracer BTC of the
181 respective tracer at the given location. The medians of the best 1,000 model simulations were used to assess the
182 agreement between our final model fits and a subset of possible curve fits. The details on the model calibration
183 procedure that we use in this work were presented in the supporting information of Gootman et al. (2020). Examples
184 of observed and fitted breakthrough curves can be found in Figures S1-S3.

185 We estimated conservative transport timescales from the transport parameters to describe the transient
186 storage timescale, $\tau_{sz} = 1/k$ [T], and the mean travel time between sites A and B, τ [T], which was computed as:

$$187 \tau = \frac{m_{1,cl}}{m_{0,cl}} \quad (3)$$

$$188 m_n = \sum_{i=1}^r \left(\frac{t_i + t_{i+1}}{2} \right)^n \left(\frac{C_i + C_{i+1}}{2} \right) (t_{i+1} - t_i) \quad (4)$$

$$189 \tau = \frac{m_{1,cl}}{m_{0,cl}} \quad (3)$$

$$m_n = \sum_{i=1}^r \left(\frac{t_i + t_{i+1}}{2} \right)^n \left(\frac{C_i + C_{i+1}}{2} \right) (t_{i+1} - t_i) \quad (4)$$

190 where $m_{0,cl}$ and $m_{1,cl}$ are the zeroth and first-centralized temporal moments of the Cl⁻ BTCs from each sampling
191 site, i is a time index, r is the total number of samples available in a BTC.

192 2.3 Estimating the transformation of Raz as a proxy for microbial respiration:

193 We used the net transformation rate coefficients of Raz, λ_{Raz} [T⁻¹], as a proxy for microbial respiration,
194 and estimated them following the work by González-Pinzón and Haggerty (2013), which derived algebraic

Commented [RGPI]: <https://doi.org/10.1515/IJNSNS.2009.10.3.273>

relationships to calculate processing rate coefficients from the transient storage model presented here in Equations 1 and 2:

$$\lambda_{Raz} = \lambda_{mcRaz} + \lambda_{tsRaz} = \frac{\ln(m_{0,Raz}^{inj}/m_{0,Raz}^{BTC})}{\tau} \left(1 + \frac{\overset{\text{dispersion term, } \Phi}{\ln(m_{0,Raz}^{inj}/m_{0,Raz}^{BTC})}}{Pe} \right) \quad (5)$$

where $m_{0,Raz}^{inj} = M_{Raz}/Q$ is the zeroth temporal moment of Raz at the injection site [$M L^{-3} T^{-1}$], M_{Raz} is the mass of Raz added to the injectate, Q is the stream discharge [$L^3 T^{-1}$]; $m_{0,Raz}^{BTC}$ is the dilution-corrected zeroth temporal moment of Raz estimated with BTC data from a sampling site; and $Pe = Lu/D$ is the Peclet number [-], which describes the relative importance of advection and dispersion in the system.

In the work by González-Pinzón and Haggerty (2013) since we can only get the use of zeroth temporal moments implied that only one processing-rate coefficient could be estimated from every observed BTC available from Equation (5), or from the direct calibration of the transient storage model, we expanded the work by González-Pinzón and Haggerty (2013). However, using to incorporate the conceptual principles proposed in the Tracer Addition for Spiraling Curve Characterization (TASCC) framework (Covino et al. 2010b), where multiple rate coefficients can be estimated from an equivalent version of Equation 5.

Briefly, TASCC uses the dynamic range of solute concentrations sampled in BTCs to characterize uptake kinetics from ambient to saturation concentrations. In TASCC, the ratio of reactive to conservative solute concentrations for every independent sample across the tracer BTCs is compared to the ratio of the concentrations of the injection solution to determine uptake metrics. If the added solutes are non-limiting or non-reactive, they will transport conservatively, and the ratio of the reactive to conservative solute concentrations will remain constant. Alternatively, if the added solutes are limiting, co-limiting or reactive, they will not transport conservatively, and the ratio of the reactive to conservative solute concentrations will change over time as a function of reactivity.

To incorporate the TASCC framework into the algebraic equation developed by González-Pinzón and Haggerty (2013) and estimate transformation rate coefficients for Raz from each pair of conservative (i.e., C_{cons}) and reactive tracer concentrations (i.e., C_{Raz}), we need to replace m_0 with C_{Raz}/C_{cons} . This guarantees that the mean value of all the processing-rate coefficients is equal to the processing-rate coefficient estimated from the zeroth temporal moment analysis of model-derived simulations from Equations (1) and (2). Accordingly:

$$\lambda_{Raz, sample} = \frac{\ln\left(\frac{C_{Raz}}{C_{cons}}\right)_{inj} - \ln\left(\frac{C_{Raz}}{C_{cons}}\right)_{BTC}}{\tau} \left(1 + \frac{\overset{\text{dispersion term, } \Phi}{\ln\left(\frac{C_{Raz}}{C_{cons}}\right)_{inj} - \ln\left(\frac{C_{Raz}}{C_{cons}}\right)_{BTC}}}{Pe} \right) \quad (6)$$

Equation 6 directly links different transport mechanisms used to explain the transport and fate of solutes (i.e., advection, dispersion, transient storage, and reactivity) with TASCC, an algorithm yielding higher information content from experimental work. We note here that alternative forms of Equation 6 can be derived for solute transport models, including additional reactions such as sorption and production. Therefore, similar new equations

227 could be derived to provide mechanistic explanations to TASC-related findings noticing hysteresis behavior in
228 nutrient uptake between the rising and falling limbs of experimental BTCs (Gibson et al. 2015; Trentman et al.
229 2015; Rodríguez-Cardona et al. 2016; Brooks et al. 2017; Day and Hall 2017).

230 Finally, from each transformation rate coefficient $\lambda_{Raz, sample}$, we also estimated an uptake (or mass
231 transfer) velocity of Raz, $V_{f_{Raz, sample}} = \lambda_{Raz, sample} \cdot h$, where h is the mean depth of the stream. Following
232 Ensign and Doyle (2006), uptake velocities represent the vertical velocity of solute molecules through the water
233 column towards the benthos and are typically used in stream ecology to normalize processing-rate coefficients by
234 the influence from contrasting discharge magnitudes to facilitate the comparison of results from small streams and
235 large rivers.

236 2.4 Statistical tests

237 We calculated standard deviations (std) based on repeated measures of the distribution of the transport
238 parameters of Equations 1 and 2 to create upper and lower boundaries of the uncertainties in our measurements (i.e.,
239 mean \pm std). Because our data were not normally distributed, we used the Mann-Whitney U nonparametric statistical
240 test to determine if there were statistically significant differences between nutrient treatments across rounds (e.g., N
241 vs. N in rounds 1 and 2), following a similar procedure in Ensign and Doyle (2006). For the Mann-Whitney U test,
242 we set our significance level (α , alpha) equal to 0.05.

243 We explored the Pearson correlation coefficient (r) matrix between the transport parameters of Equations 1
244 and 2, and associated metrics, to establish direct ($r > 0.1$), inverse ($r < -0.1$), and non-existent correlations ($-0.1 < r$
245 < 0.1) (Bowley 2008). We classified the strength of the correlations as uncorrelated ($0 < r < |0.1|$), weakly correlated
246 ($|0.1| < r < |0.5|$), moderately correlated ($|0.5| < r < |0.8|$), strongly correlated ($|0.8| < r < |1.0|$), and included p-values for
247 each correlation.

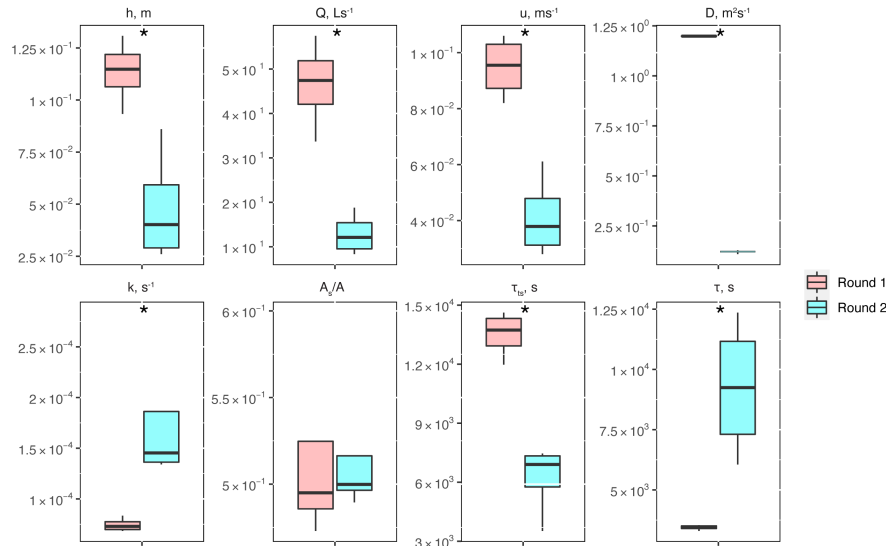
248 Lastly, we tested differences in mean values of the transport parameters of Equations 1 and 2, and
249 associated metrics, between nutrient treatments within each experimental round (e.g., N vs. N+C vs. N+P vs.
250 C+N+P in round 1) using the Student's t -test based on deviation from the group's mean value (Blair et al. 1980).

251 3 Results and Discussion

252 3.1 Conservative transport and metrics of physical controls

253 Between experimental rounds 1 and 2, stream depth (h) and discharge (Q) decreased, causing significant
254 differences in stream velocity (u), dispersion (D), mass-transfer rate coefficients (k), transient storage time scales
255 (τ_{TS}) and mean travel times (τ) (Figure 2). The only parameter that did not show significant differences was the
256 relative contribution of the main channel to storage zone areas, A_s/A .

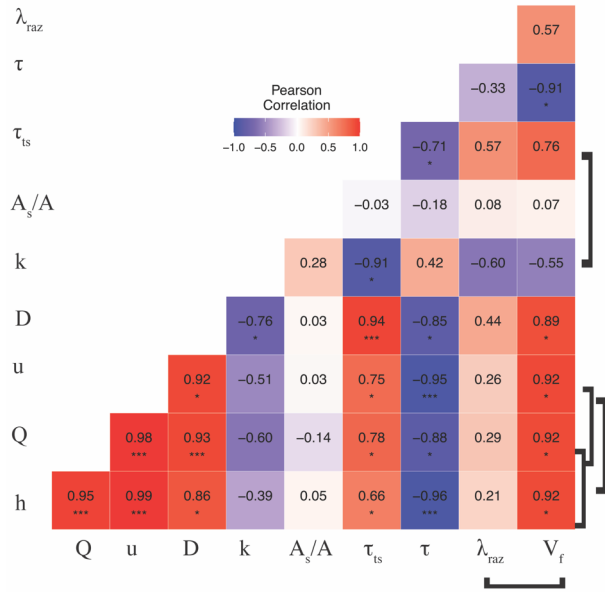
257



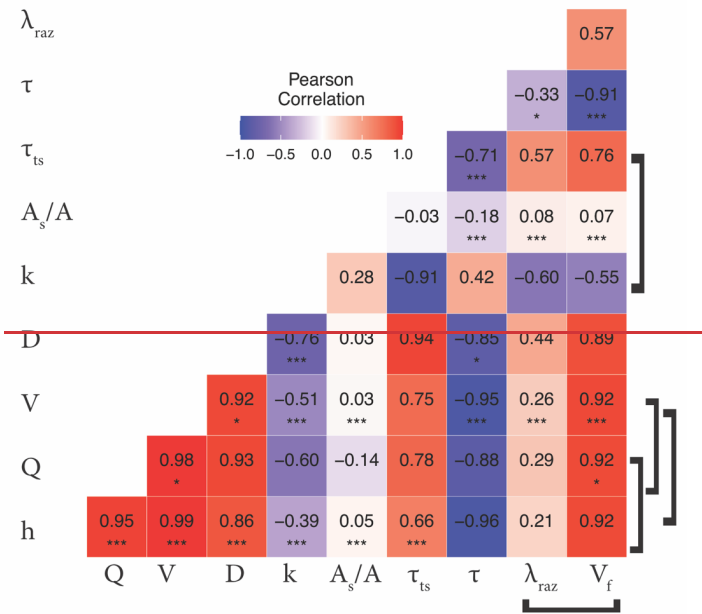
258
 259 **Figure 2:** Conservative transport parameters and metrics of physical controls estimated for the two experimental rounds:
 260 stream depth (h), stream velocity (u), dispersion (D), mass transfer rate coefficients (k), the ratio of transient storage-
 261 dominated to advection-dominated compartments (A_s/A), transient storage time scales (τ_{TS}) and mean travel times (τ).
 262 Asterisks represent statistical differences in magnitudes for rounds 1 and 2 with $p < 0.05$ (*) based on the Mann-Whitney U
 263 nonparametric statistical test.
 264
 265

266 The correlation matrix between parameters and metrics (Figure 3) shows that Q (and interrelated quantities
 267 h and u), D , and τ_{TS} were all directly correlated (from moderately to strongly). Mean travel times between sites, τ ,
 268 were directly and weakly correlated with k and the ratio A_s/A , and inversely correlated (from weakly to strongly)
 269 with the rest of the conservative transport parameters and metrics. Finally, the ratio A_s/A was generally uncorrelated
 270 or weakly correlated with other quantities. Even though the correlations of some interdependent quantities are
 271 known to be spurious, e.g., Q vs. u and λ_{Raz} vs. V_{fRaz} (González-Pinzón et al. 2015), we included all relevant
 272 measured and modeled quantities in Figure 3 to allow readers to explore different data pairs. For clarity, we
 273 differentiate with brackets all known spurious correlations. Note that we did not flag the correlation between A_s/A
 274 and Q (and their interrelated quantities h and u) as spurious because the ratio of areas is an indicator of the relative
 275 volume-based contribution from advection-dominated to transient storage-dominated compartments, instead of
 276 actual estimates of cross-sectional areas (Kelleher et al. 2013; González-Pinzón et al. 2013; Knapp and Kelleher
 2020).

277



278



279

280 Figure 3: Pearson correlation coefficient (r) heatmap for the mean values of the transport parameters and metrics for
281 each stoichiometric treatment during rounds 1 and 2. Brackets link known spurious correlations. Asterisks represent
282 significant differences in magnitudes between parameters with $p < 0.05$ (*), and $p < 0.001$ (***) based on the Pearson
283 Correlation.

284
285 One of the metrics of interest in stream reactive-transport modeling is the transient storage timescale ($\tau_{ts} =$
286 $1/k$), which quantifies the exposure that solutes have to biological communities in metabolically active transient
287 storage zones. In our study site, τ_{ts} decreased one order of magnitude from round 1 to round 2, and were comparable
288 to the range of values observed in other studies involving forested mountain streams (Valett et al. 1996; Hall et al.
289 2002). Due to the geomorphology of the stream, which is characterized by ~~steep longitudinal and valley slopes~~, pool
290 and riffle sequences, ~~and but steep longitudinal and valley slopes~~ and shallow bedrock, transient storage was
291 expected to occur mainly in the main channel (Fields and Dethier 2019; Barnhart et al. 2021; Emanuelson et al.
292 2022). As flow receded from round 1 to round 2, we observed the disconnection of in-stream pools contributing to
293 transient storage, which explains the direct correlation between discharge and transient storage timescales. Another
294 indication of the dominant contribution of in-stream pools to total transient storage is the lack of change of A_s/A
295 with discharge. ~~Since A is expected to vary proportional with discharge (i.e., $Q = A \cdot u$), a constant A_s/A which~~
296 suggests that the contribution of transient storage-dominated (i.e., A_s) ~~and advection-dominated~~ compartments (i.e.,
297 A) ~~also varied proportionally over changes in~~with discharge.

298 3.2 Raz transformation (a proxy for respiration) as a function of physical controls

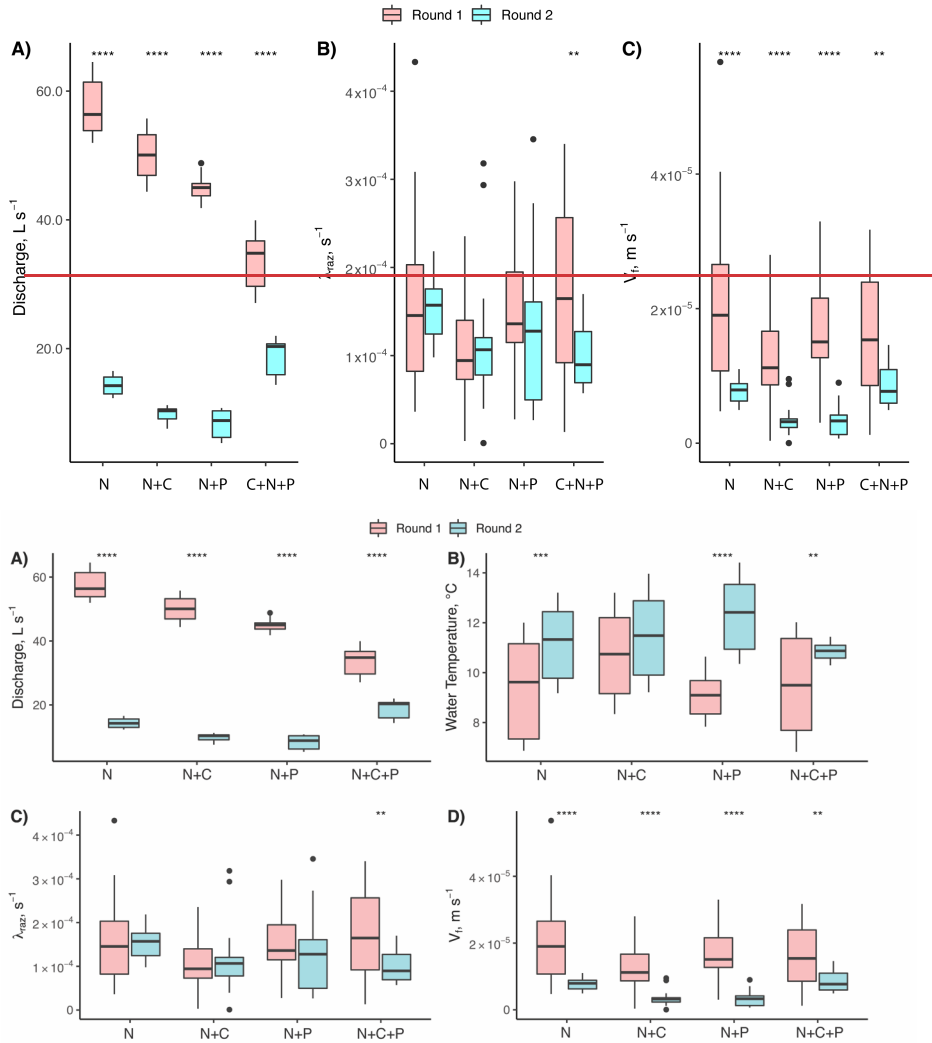
299 Our results indicate that the ~~mean values of the~~ transformation rate coefficient of Raz (λ_{Raz}) ~~was/were~~
300 directly and moderately correlated with the transient storage timescale (τ_{ts}), as other studies on reactive transport
301 have shown (Valett et al. 1996; Hall et al. 2002; Gomez et al. 2012; Zarnetske et al. 2012; Kiel and Bayani Cardenas
302 2014; Gootman et al. 2020). ~~The mean values of~~ Mean λ_{Raz} values were directly and weakly correlated with
303 discharge (Q) (also depths h and velocities u) and dispersion (D), and directly and moderately correlated with τ_{ts} .
304 ~~The transformation rate coefficient of Raz Mean~~ (λ_{Raz}) values were inversely and weakly correlated with mean
305 travel times (τ), and inversely and moderately correlated with mass-transfer rate coefficients (k) (Figure 3). Raz
306 uptake velocities ($V_{f,Raz}$) showed spurious, direct and strong correlations with discharge (Q) (also h and u), strong
307 correlations with dispersion (D) and transient storage timescales (τ_{ts}), and strong indirect correlations with mean
308 travel times (τ) and k (moderate). Finally, both λ_{Raz} and $V_{f,Raz}$ were uncorrelated with A_s/A . Unlike studies where
309 an increased transient storage timescale (τ_{ts}) is mainly associated with slower hyporheic flows due to lower
310 discharges (Q) (Zarnetske et al. 2007; Schmid et al. 2010), τ_{ts} in our study site increased with Q because the
311 geomorphology of the channel and the valley favored in-stream transient storage in ~~lateral~~ pools (Jackson et al.
312 2012, 2013, 2015). ~~Similar declines in transient storage with falling discharge have been observed in other streams~~
313 ~~with comparable geomorphic characteristics (Covino et al. 2010a; Emanuelson et al. 2022), however, the absence of~~
314 ~~concurrent declines in respiration suggest biological control by some other mechanism, and the metabolically active~~
315 ~~biofilms available there may have prompted the transformation of Raz (Haggerty et al. 2014; Peralta-Maraver et al.~~
316 ~~2018). Consistently, when stream flows recede in these types of streams, the subsequent disconnection of parts of~~

317 the channel causes a decline in transient storage and metabolism (Covino et al. 2010a; Emanuelson et al. 2022). Hall
318 et al. (2002) found similar results in a study of thirteen streams, where changes in stream width and depth primarily
319 drove variations in transient storage timescales.

320 3.3 Raz transformation (a proxy for respiration) as a function of physical and stoichiometric controls

321 Our results suggest no significant changes in respiration despite significant differences in discharge (Q),
322 temperature, and nutrient treatments. Between experimental rounds, the mean values of Q (and h and u by
323 extension) and temperature (except for N+C) were statistically different for each treatment comparison (Figure 4A).
324 For λ_{Raz} , we only found statistical differences between rounds for the C+N+P treatments (Figure 4B4C). Due to the
325 large influence of Q on the uptake velocity of Raz ($V_{f_{Raz}}$) through stream depth (h), the statistical differences
326 between rounds seen for Q were also seen for $V_{f_{Raz}}$ (Figure 4C4D).
327

328



329

330

331

332

333

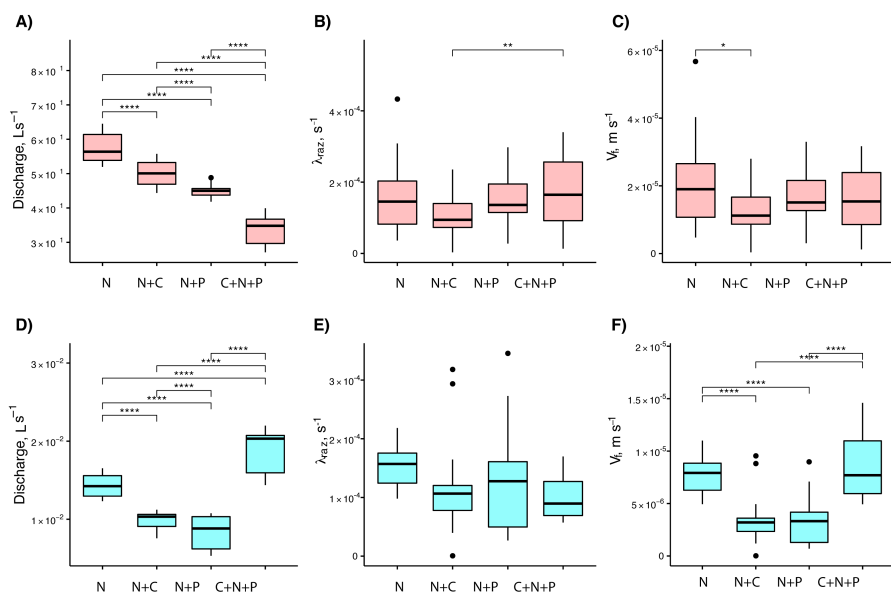
334

335

336

Figure 4: Comparison of A) stream discharge values recorded at the gaging station, B) stream water temperatures, C) transformation rate coefficients of resazurin (λ_{Raz}) resulting from Equation 6, and associated D) uptake velocities of resazurin ($V_{fRaz} = \lambda_{Raz} h$) estimated for each experimental nutrient treatment addition during rounds 1 and 2. Due to the large influence of Q on the uptake velocity of Raz (V_{fRaz}) through stream depth (h), most of the statistical differences between rounds seen for Q were also seen for V_{fRaz} . Asterisks represent significant differences in magnitudes between rounds with $p < 0.01$ (**), and $p < 0$ (****) based on the Mann-Whitney U nonparametric statistical test.

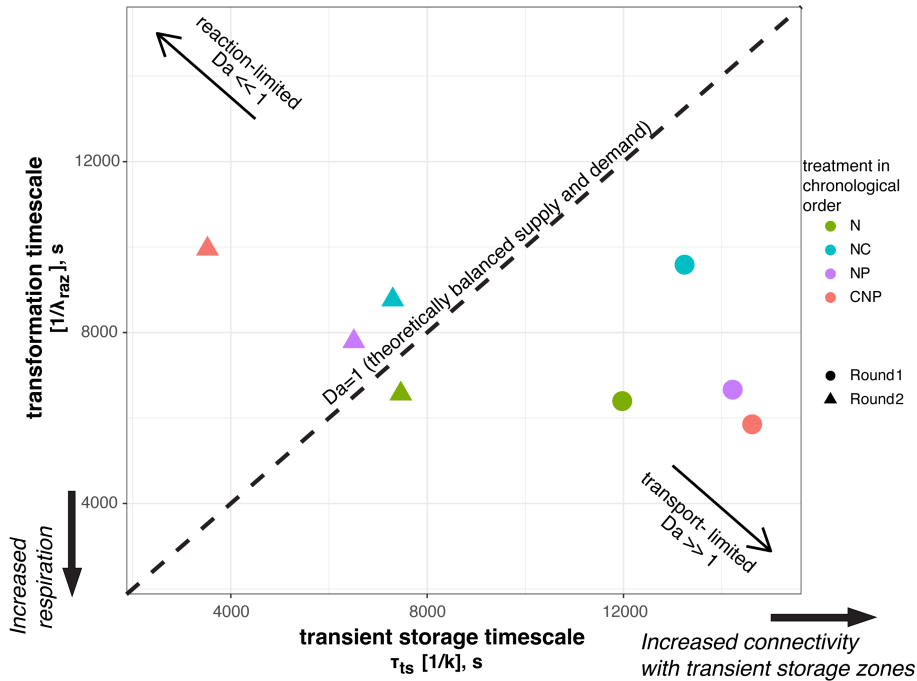
337 When looking at the data collected from each round, we found that mean Q values were statistically
 338 different across nutrient treatments (Figures 5A and 5D). For mean λ_{Raz} values, the only treatments with statistical
 339 differences were the N+C and C+N+P from round 1 (Figures 5B and 5E). Finally, $V_{f,Raz}$ mean values were only
 340 statistically different for the N vs N+C treatments for round 1, and for all but the N+C vs N+P and N vs C+N+P
 341 treatments for round 2 (Figures 5C and 5F).
 342



343 **Figure 5:** Comparison of stream discharges (A and D), transformation rate coefficients of resazurin (λ_{Raz}) (B and E), and
 344 uptake velocities of resazurin ($V_{f,Raz}$) (C and F) across treatments for round 1 (top row) and 2 (bottom row). Due to the
 345 large influence of Q on the uptake velocity of Raz ($V_{f,Raz}$) through stream depth (h), most of the statistical differences
 346 between rounds seen for Q were also seen for $V_{f,Raz}$. Asterisks represent significant differences in magnitudes for
 347 treatments N, N+C, N+P, and C+N+P with $p < 0.05$ (*), $p < 0.01$ (**), and $p < 0$ (****) based on the Mann-Whitney U
 348 nonparametric statistical test.
 349

350 For each of the eight nutrient injections, we related the mean transient storage timescales, τ_{ts} , which
 351 indicate exposure times between solutes and microbial communities, and the mean transformation timescales of Raz,
 352 $1/\lambda_{Raz}$, which indicate respiration (Figure 6). This Damköhler-based analysis allows us to visualize the interplay
 353 between physical, biological, and stoichiometric controls in the stream. We found that the range of variation of the
 354 mean transient storage timescales was three times greater than that of the mean transformation timescales. This
 355 suggests that the changes brought by our stoichiometric controls (color-coded in Figure 6) may have contributed to
 356 buffer changes in microbial respiration. In round 1, all the stoichiometric treatments resulted in transport-limited
 357 conditions due to the high values of τ_{ts} , i.e., the average particle of Raz that entered a metabolically active
 358

359 compartment underwent transformation and more Raz could have been transformed if it had been available. Thus, in
 360 round 1, respiration was high relative to the supply of solutes to the metabolically active transient storage zones. In
 361 round 2, all stoichiometric treatments, except N, resulted in reaction-limited conditions, i.e., the average particle of
 362 Raz entering a metabolically active compartment left it without undergoing transformation. Thus, in round 2,
 363 respiration was slow relative to the exposure of solutes to microbial communities.
 364
 365



366 Figure 6: Mean reaction and transient storage timescales for each nutrient treatment. The Damköhler, $Da =$
 367 transient storage timescale/ transformation timescale, indicates reaction-limited and transport-limited conditions.
 368
 369

370 **3.4 How is microbial respiration controlled by hydrologic exchange vs. stoichiometric conditions (i.e., supply**
 371 **of C, N, and P)?**

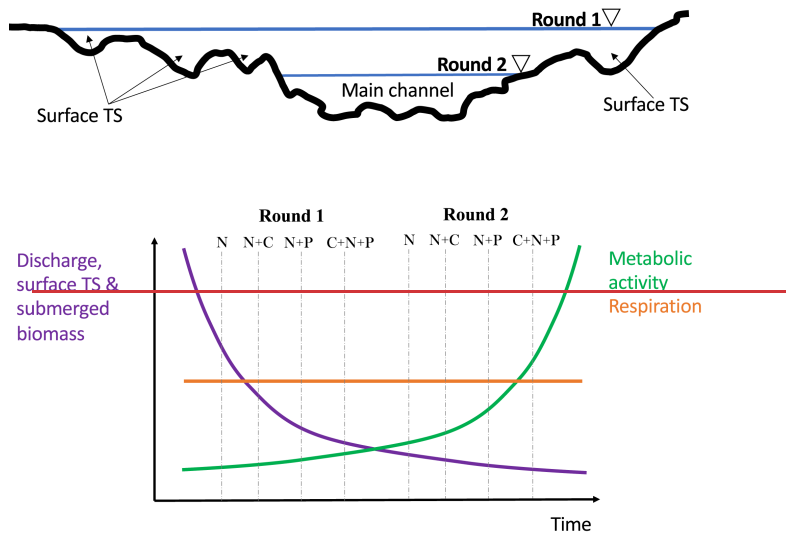
372 We characterized microbial respiration with the transformation timescale of Raz, $1/\lambda_{Raz}$; the extent of
 373 hydrologic exchanges with the transient storage timescale, τ_{TS} , and the relative size of the main channel and
 374 transient storage areas, A_s/A ; and stoichiometric conditions with our controlled nutrient additions (i.e., N, N+C,
 375 N+P, and C+N+P treatments). The most salient findings indicate that a) discharge (Q) changed significantly
 376 between rounds (Figure 4a) and across stoichiometric treatments (Figure 5a, 5d), and was directly and moderately

377 correlated with τ_{TS} and uncorrelated with A_s/A (Figure 3), suggesting that most transient storage occurred in the
378 ~~side~~lateral pools in the channel, which increased in quantity and extent proportionally with Q , and b) the respiration
379 activity indicated by λ_{Raz} remained similar between rounds with significantly different Q (Figure 4b), and across
380 controlled stoichiometric treatments also featuring different Q (Figure 5b, 5e). Thus, we observed that respiration
381 remained largely unchanged or constant with varying physical and stoichiometric conditions, ~~as we summarized in~~
382 ~~Figure 7.~~

383 Several hypotheses may explain the invariant respiration observed between experimental rounds and
384 treatments. First, tradeoffs in metabolic rates may have occurred as the stream shifted from high to low flows. At
385 high flows during late June and early July, lateral pools in the main channel were inundated, and transient storage
386 timescales likely associated with these pools were high. Under these conditions, the observed respiration was
387 probably supported by low levels of processing in the hyporheic zone due to the prevalence of bedrock substrate and
388 relatively low respiration from benthic biomass due to scour from high flows (Francoeur and Biggs 2006; Katz et al.
389 2018). However, the combination of longer transient storage timescales and an expanded total surface area resulted
390 in moderate total respiration. In contrast, during the low flows seen in the second round of injections, surface area,
391 and transient storage timescales were decreased due to the contraction of the channel. Under these conditions,
392 biomass increased likely due to decreased scour and increased stability (Francoeur and Biggs 2006; Katz et al. 2018;
393 Cargill et al. 2021), increased water temperatures (Perkins et al. 2012), and increased processing of autochthonous
394 carbon (Wagner et al. 2017) (Figure S4). This may have supported elevated areal metabolic rates in benthic
395 biofilms (Battin et al. 2016), maintaining relatively constant respiration levels with respect to the first round of
396 injections.

397 An alternative hypothesis to explain the consistency of the observed respiration values is that some other
398 factor constraints respiration values within a narrow range. For example, the limitation of a key nutrient or metabolic
399 resource may constrain respiration. While we designed the experiments to relieve stoichiometric constraints, it is
400 possible that the quantities of C, N, and P in the injectate we were logistically able to introduce to the stream were
401 insufficient to overcome demand. Also, the form of the resources may not have been readily available to
402 communities adapted to these locals, as stream microbial communities most efficiently process the forms and
403 diversity of dissolved organic matter found in their native habitats, and they express extracellular enzymes in ratios
404 appropriate to acquire limiting nutrients (Hill et al. 2012; Lane et al. 2012; Wilhelm et al. 2015; Logue et al. 2016).
405 Given that each experimental round lasted only one week, in the absence of stoichiometric manipulations, we would
406 have expected to see changes in microbial respiration proportional to the constraints imposed by the physical
407 controls in the stream. This expectation is based on the assumption that there are insignificant changes to the
408 microbial composition of a stream during any given week. Consequently, the disconnection of surface transient-
409 storage zones with microbial biomass due to the marked flow recessions should have resulted in reduced
410 transformation of Raz, i.e., reduced respiration (González-Pinzón et al. 2012, 2014; Knapp et al. 2017, 2018).
411 Within this context, the constant respiration that we observed in our study may have resulted from counterbalanced
412 interactions between flow reductions, which decreased surface transient storage and the amount of biomass
413 connected to the stream, and an increase in metabolic activity likely prompted by the removal of nutrient limitations

414 from our sequential additions of N, N+C, N+P, and C+N+P (Figure 7). This is supported by evidence showing that
 415 microbial biofilms operate as rate-limited systems, where solutes and particulates can remain stored longer and be
 416 utilized later than the resources transported in the main channel (Battin et al. 2003, 2016; Merchant and Helmann
 417 2012). Therefore, even if our nutrient additions were carried out every other day to allow the stream to return to
 418 ambient conditions, nutrients might have become increasingly more abundant inside connected biofilms,
 419 progressively contributing to reducing nutrient limitations. Simply put, while less biomass contributed to respiration
 420 when side pools became disconnected through flow reductions, the connected biofilms may have been more
 421 metabolically active, causing constant respiration activities.
 422



423
 424 **Figure 7. Conceptual diagram explaining constant stream respiration in Como Creek: the study featured flow recession**
 425 **and two rounds of stoichiometric treatments: N, N+C, N+P, and C+N+P.**
 426

427 Our findings support the idea that transient storage timescales alone could be a weak predictor of stream
 428 respiration due to the relevance of local and dynamic variations in stoichiometric conditions. In previous studies,
 429 transient storage and nutrient uptake have presented contradictory relationships, which we summarize below.

430 *Inconclusive relationships:* Martí et al. (1997) did not find correlations between NH_3 uptake length and
 431 A_s/A in a desert stream using data from eight tracer injections. Webster et al. (2003) did not find statistically
 432 significant relationships between NH_4 uptake and A_s/A using the 11-stream LINX-I dataset that included arctic to
 433 tropical streams. From thirty seven injections conducted in thirteen streams at Hubbard Brook Experimental Forest
 434 (HBEF), Hall et al. (2002) found weak correlations ($R^2=0.14-0.35$) between transient storage parameters and NH_4
 435 demand. Using data from seven streams in New Zealand, Niyogi et al. (2004) did not find significant correlations

436 between soluble reactive phosphorous (P-SRP), NO₃ uptake velocities, and A_s/A. Bukaveckas (2007) reported an
437 indefinite relationship between transient storage and NO₃ and P-SRP retention efficiencies from tracer injections in a
438 reference (N=13 injections), a channelized (N=14 injections), and a restored (N=17 injections) stream reach in the
439 midwestern US. Lastly, the LINX-II dataset from ¹⁵N-NO₃ injections in 72 streams located in eight regions of the
440 US showed no relationship between NO₃ uptake and the fraction of median travel time due to transient storage
441 (F_{med}^{200}) (Hall et al. 2009).

442 *Weak to moderate relationships:* Thomas et al. (2003) showed that transient storage accounted for 44% to
443 49% of NO₃ retention measured by ¹⁵N in a small headwater stream in North Carolina. Mulholland et al. (1997)
444 found larger PO₄ uptake rates in a stream with higher transient storage, when they compared two forested streams.
445 Ensign and Doyle (2005) found an increase in A_s/A and the uptake velocities for NH₄ and PO₄ after the addition of
446 flow baffles to two streams. Lautz and Siegel (2007) found a modest correlation (R²=0.44) between NO₃ retention
447 efficiency and transient storage in the Red Canyon Creek watershed, WY.

448 *Strong relationships:* Valett et al. (1996) found a strong correlation (R²=0.77) between transient storage
449 and NO₃ retention in three first-order streams in New Mexico. From nine tracer injections in two urban streams in
450 the eastern US, Ryan et al. (2007) found strong relationships between P-SRP retention and transient storage metrics
451 ($k, A_s/A$; R²>0.84) when the variables were measured in different seasons. Sheibley et al. (2014) observed that the
452 retention of NO₃ in seven agricultural streams in the US was positively correlated with A_s/A and the average water
453 flux through the storage zone per unit length of stream ($q_s = kA$), and negatively correlated with the transient
454 storage timescale (τ_{ts}). However, they found no significant correlation between NH₄⁺ and SRP retention and
455 transient storage metrics.

456 The studies referenced above were ~~done-performed~~ in streams with contrasting physical, chemical, and
457 biological conditions. Together, they offer a broader perspective on the inconsistent relationship between transient
458 storage metrics and metabolic processing. Those studies do not feature co-injections of C, N, and P macronutrients
459 (e.g., N+C, N+P, N+C+P), even while some tracked ambient processing rates of more than one nutrient. Therefore,
460 they generally represent solute-specific analyses, where the uptake of one nutrient at a time was analyzed and, thus,
461 did not account for stoichiometric controls on nutrient uptake (~~however, see Tromboni et al. (2018) for an~~
462 ~~example of recent trend changes in this research area.~~ ~~On the contrary~~By combining both transport and
463 stoichiometric analyses, our study offers evidence ~~suggesting~~that stoichiometric controls ~~have an ambiguous~~
464 ~~relationship to can be as important as physical controls in establishing~~reach-scale metabolic activities, ~~explaining~~
465 ~~why transient storage timescales alone could be a weak predictor of stream metabolic processes, and that further~~
466 ~~investigations should be conducted using greater quantities and types of resources.~~

467 4 Conclusions

468 We conducted two rounds of four stoichiometric treatments (i.e., N, C+N, N+P, and C+N+P) in a
469 headwater stream in Colorado to quantify changes to stream respiration during flow recession and answer the
470 question: *How is respiration controlled by hydrologic exchange vs. stoichiometric conditions (i.e., supply of C, N,*

471 *and P*)? We found that discharge changed significantly between rounds and across stoichiometric treatments, and
472 that it was directly and moderately correlated with transient storage timescales but uncorrelated with the ratio of
473 contributions from advection-dominated to transient storage-dominated compartments (i.e., A_S/A). This suggests
474 that most transient storage occurred in side-lateral pools within the main channel, which increased in quantity and
475 extent proportionally with discharge. We also found that respiration remained similar despite significant changes in
476 discharge and stoichiometric treatments. Our results contradict the notion that hydrologic transport alone is a
477 dominant control on biogeochemical processing, and suggest that complex interactions between hydrology, resource
478 supply, and biological community function are responsible for driving in-stream respiration. as longer transient
479 storage timescales were not uniquely associated with increased respiration in our study. Interestingly, our results
480 suggest that the sequential stoichiometric treatments that we conducted over the two rounds of experiments
481 counterbalanced the controls imposed by hydrologic transport, consistently resulting in insignificant changes in
482 stream respiration between rounds and treatments. Together, we saw that residence time alone could be a weak
483 predictor of stream respiration due to the relevance of local and dynamic variations in stoichiometric conditions. Our
484 results offer a plausible explanation for the lack of consistency in reported relationships between transient storage
485 and in-stream nutrient processing from prior studies.

486 **Author contribution:** RGP, TC, KS, and MG secured the funding for this research. All co-authors designed carried
487 out the experiments. JD and RGP processed Raz-Rru samples, performed solute transport simulations, statistical
488 analyses, and prepared the manuscript with input from all co-authors. DVH supported the contextualization of
489 hydrological and ecological interactions. All co-authors approved the final version of the manuscript.

490 **Competing interests:** The authors declare no competing interests.

491 **Acknowledgments**

492 The National Science Foundation provided funding support through grants NSF EAR-1642399, NSF EAR-
493 1642368, NSF EAR-1642402, NSF EAR-1642403, and NSF 1914490. We thank Karin Emanuelson, Jackie
494 Randell, Erin Jenkins, Tristan Weiss, and Melissa Pinzon for their field and laboratory assistance.

495 **Data availability:**

496 The data used in his article can be found in the CUAHSI HydroShare repository. Gonzalez-Pinzon, R. (2022).
497 Resazurin tracer data from experiments in Colorado (2018) and Iowa (2019),
498 HydroShare, <http://www.hydroshare.org/resource/50ae3c59bebe4cb383e31408a0c10012>

499
500
501
502

503 **References**

- 504 Barnhart, T. B., J. Vukomanovic, P. Bourgeron, and N. P. Molotch. 2021. Future land cover and
505 climate may drive decreases in snow wind-scour and transpiration, increasing streamflow
506 at a Colorado, USA headwater catchment. *Hydrol. Process.* **35**: e14416.
507 doi:10.1002/hyp.14416
- 508 Battin, T. J., K. Besemer, M. M. Bengtsson, A. M. Romani, and A. I. Packmann. 2016. The
509 ecology and biogeochemistry of stream biofilms. *Nat. Rev. Microbiol.* **14**: 251–263.
510 doi:10.1038/nrmicro.2016.15
- 511 Battin, T. J., L. A. Kaplan, J. D. Newbold, and C. M. E. Hansen. 2003. Contributions of
512 microbial biofilms to ecosystem processes in stream mesocosms. *Nature* **426**: 439–442.
513 doi:10.1038/nature02152
- 514 Blair, R. C., J. J. Higgins, S. Journal, and N. Winter. 1980. A Comparison of the Power of
515 Wilcoxon ' s Rank-Sum Statistic to That of Student ' s t Statistic under Various
516 Nonnormal Distributions Published by : American Educational Research Association and
517 American Statistical Association Stable URL : <https://www.jstor.org/stable/1164905>
518 REFERENCES Linked references are available on JSTOR for this article : reference #
519 references _ tab _ contents You may need to log in to JSTOR to access the linked
520 references . **5**: 309–335.
- 521 Blume, E., M. Bischoff, J. M. Reichert, T. Moorman, A. Konopka, and R. F. Turco. 2002.
522 Surface and subsurface microbial biomass, community structure and metabolic activity as
523 a function of soil depth and season. *Appl. Soil Ecol.* **20**: 171–181. doi:10.1016/S0929-
524 1393(02)00025-2
- 525 Bowley, A. L. 2008. The Standard Deviation of the Correlation Coefficient Author (s) : A . L .
526 Bowley Source : *Journal of the American Statistical Association* , Vol . 23 , No . 161 (
527 Mar . , 1928) , pp . 31- Published by : American Statistical Association Stable URL :
528 <http://www.jstor.org/stable/233134> . *J. Am. Stat. Assoc.* **23**: 31–34.
- 529 Brooks, S. C., C. C. Brandt, and N. A. Griffiths. 2017. Estimating uncertainty in ambient and
530 saturation nutrient uptake metrics from nutrient pulse releases in stream ecosystems.
531 *Limnol. Oceanogr. Methods* **15**: 22–37. doi:10.1002/lom3.10139
- 532 Bukaveckas, P. A. 2007. Effects of Channel Restoration on Water Velocity, Transient Storage,
533 and Nutrient Uptake in a Channelized Stream. *Environ. Sci. Technol.* **41**: 1570–1576.
534 doi:10.1021/es061618x
- 535 Cardenas, M. B., J. L. Wilson, and V. A. Zlotnik. 2004. Impact of heterogeneity, bed forms, and
536 stream curvature on subchannel hyporheic exchange. *Water Resour. Res.* **40**: 1–14.
537 doi:10.1029/2004WR003008
- 538 Cargill, S. K., C. Segura, S. R. Villamizar, and D. R. Warren. 2021. The influence of lithology
539 on stream metabolism in headwater systems. *Ecohydrology* **14**. doi:10.1002/eco.2284
- 540 Covino, T. P., B. McGlynn, and M. Baker. 2010a. Separating physical and biological nutrient
541 retention and quantifying uptake kinetics from ambient to saturation in successive
542 mountain stream reaches. *J. Geophys. Res. Biogeosciences* **115**: 1–17.
543 doi:10.1029/2009JG001263
- 544 Covino, T. P., and B. L. McGlynn. 2007. Stream gains and losses across a mountain-to-valley
545 transition: Impacts on watershed hydrology and stream water chemistry. *Water Resour.*
546 *Res.* **43**: 1–14. doi:10.1029/2006WR005544

- 547 Covino, T. P., B. L. McGlynn, and R. A. Mcnamara. 2010b. Tracer Additions for Spiraling Curve
548 Characterization (TASCC): Quantifying stream nutrient uptake kinetics from ambient to
549 saturation. *Limnol. Oceanogr. Methods* 484–498. doi:10.4319/lom.2010.8.484
- 550 Covino, T. P., B. McGlynn, and J. Mallard. 2011. Stream-groundwater exchange and hydrologic
551 turnover at the network scale. *Water Resour. Res.* 47: 1–11. doi:10.1029/2011WR010942
- 552 Dallan, E., P. Regier, A. Marion, and R. González-Pinzón. 2020. Does the Mass Balance of the
553 Reactive Tracers Resazurin and Resorufin Close at the Microbial Scale? *J. Geophys. Res.*
554 *Biogeosciences* 125: 1–10. doi:10.1029/2019JG005435
- 555 Day, N. K., and R. O. Hall. 2017. Ammonium uptake kinetics and nitrification in mountain
556 streams. *Freshw. Sci.* 36: 41–54. doi:10.1086/690600
- 557 Emanuelson, K., T. P. Covino, A. S. Ward, J. Dorley, and M. N. Gooseff. 2022. Conservative
558 solute transport processes and associated transient storage mechanisms: Comparing
559 streams with contrasting channel morphologies, land use and land cover. *Hydrol. Process.*
560 36.
- 561 Ensign, S. H., and M. W. Doyle. 2005. In-channel transient storage and associated nutrient
562 retention: Evidence from experimental manipulations. *Limnol. Oceanogr.* 50: 1740–1751.
563 doi:10.4319/lo.2005.50.6.1740
- 564 Ensign, S. H., and M. W. Doyle. 2006. Nutrient spiraling in streams and river networks. *J.*
565 *Geophys. Res. Biogeosciences* 111. doi:10.1029/2005jg000114
- 566 Fields, J. F., and D. P. Dethier. 2019. From on high: Geochemistry of alpine springs, Niwot
567 Ridge, Colorado Front Range, USA. *Hydrol. Process.* 33: 1756–1774.
568 doi:10.1002/hyp.13436
- 569 Francoeur, S. N., and B. J. F. Biggs. 2006. Short-term Effects of Elevated Velocity and Sediment
570 Abrasion on Benthic Algal Communities. *Hydrobiologia* 561: 59–69.
571 doi:10.1007/s10750-005-1604-4
- 572 Gelman, A., and D. B. Rubin. 1992. Inference from Iterative Simulation Using Multiple
573 Sequences. *Stat. Sci.* 7. doi:10.1214/ss/1177011136
- 574 Gibson, C. A., C. M. O'Reilly, A. L. Conine, and S. M. Lipshutz. 2015. Nutrient uptake
575 dynamics across a gradient of nutrient concentrations and ratios at the landscape scale. *J.*
576 *Geophys. Res. Biogeosciences* 120: 326–340. doi:10.1002/2014JG002747
- 577 Gomez, J. D., J. L. Wilson, and M. B. Cardenas. 2012. Residence time distributions in sinuosity-
578 driven hyporheic zones and their biogeochemical effects. *Water Resour. Res.* 48: 1–17.
579 doi:10.1029/2012WR012180
- 580 González-Pinzón, R., J. Dorley, J. Singley, K. Singha, M. Gooseff, and T. Covino. 2022. TIPT:
581 The Tracer Injection Planning Tool. *Environ. Model. Softw.* 156: 105504.
582 doi:10.1016/j.envsoft.2022.105504
- 583 González-Pinzón, R., and R. Haggerty. 2013. An efficient method to estimate processing rates in
584 streams. *Water Resour. Res.* 49: 6096–6099. doi:10.1002/wrcr.20446
- 585 González-Pinzón, R., R. Haggerty, and A. Argerich. 2014. Quantifying spatial differences in
586 metabolism in headwater streams. *Freshw. Sci.* 33: 798–811. doi:10.1086/677555
- 587 González-Pinzón, R., R. Haggerty, and M. Dentz. 2013. Scaling and predicting solute transport
588 processes in streams. *Water Resour. Res.* 49: 4071–4088. doi:10.1002/wrcr.20280
- 589 González-Pinzón, R., R. Haggerty, and D. D. Myrold. 2012. Measuring aerobic respiration in
590 stream ecosystems using the resazurin-resorufin system. *J. Geophys. Res. Biogeosciences*
591 117: 1–10. doi:10.1029/2012JG001965

- 592 González-Pinzón, R., J. Mortensen, and D. Van Horn. 2015. Comment on “Solute-specific
593 scaling of inorganic nitrogen and phosphorus uptake in streams” by Hall et al. (2013).
594 *Biogeosciences* **12**: 5365–5369. doi:10.5194/bg-12-5365-2015
- 595 González-Pinzón, R., M. Peipoch, R. Haggerty, E. Martí, and J. H. Fleckenstein. 2016.
596 Nighttime and daytime respiration in a headwater stream. *Ecohydrology* **9**: 93–100.
597 doi:10.1002/eco.1615
- 598 Gooseff, M. N., K. E. Bencala, D. T. Scott, R. L. Runkel, and D. M. McKnight. 2005. Sensitivity
599 analysis of conservative and reactive stream transient storage models applied to field data
600 from multiple-reach experiments. *Adv. Water Resour.* **28**: 479–492.
601 doi:10.1016/j.advwatres.2004.11.012
- 602 Gooseff, M. N., D. M. McKnight, R. L. Runkel, and J. H. Duff. 2004. Denitrification and
603 hydrologic transient storage in a glacial meltwater stream, McMurdo Dry Valleys,
604 Antarctica. *Limnol. Oceanogr.* **49**: 1884–1895. doi:10.4319/lo.2004.49.5.1884
- 605 Gootman, K. S., R. G. Pinzón, J. L. A. Knapp, V. Garayburu-Caruso, and J. Cable. 2020.
606 Spatiotemporal Variability in Transport and Reactive Processes Across a First - to Fifth -
607 Order Fluvial Network Water Resources Research. 1–18. doi:10.1029/2019WR026303
- 608 Hall, R. J. O., E. S. Bernhardt, and G. E. Likens. 2002. Relating nutrient uptake with transient
609 storage in forested mountain streams. *Limnol. Oceanogr.* **47**: 255–265.
610 doi:10.4319/lo.2002.47.1.0255
- 611 Hall, R. O., J. L. Tank, D. J. Sobota, and others. 2009. Nitrate removal in stream ecosystems
612 measured by 15N addition experiments: Total uptake. *Limnol. Oceanogr.* **54**: 653–665.
613 doi:10.4319/lo.2009.54.3.0653
- 614 Harvey, J. W., J. K. Böhlke, M. A. Voytek, D. Scott, and C. R. Tobias. 2013. Hyporheic zone
615 denitrification: Controls on effective reaction depth and contribution to whole-stream
616 mass balance. *Water Resour. Res.* **49**: 6298–6316. doi:10.1002/wrcr.20492
- 617 Harvey, J. W., J. E. Saiers, and J. T. Newlin. 2005. Solute transport and storage mechanisms in
618 wetlands of the Everglades, south Florida. *Water Resour. Res.* **41**.
619 doi:10.1029/2004WR003507
- 620 Hill, B. H., C. M. Elonen, L. R. Seifert, A. A. May, and E. Tarquinio. 2012. Microbial enzyme
621 stoichiometry and nutrient limitation in US streams and rivers. *Ecol. Indic.* **18**: 540–551.
622 doi:10.1016/j.ecolind.2012.01.007
- 623 Jackson, T. R., S. V. Apte, R. Haggerty, and R. Budwig. 2015. Flow structure and mean
624 residence times of lateral cavities in open channel flows: influence of bed roughness and
625 shape. *Environ. Fluid Mech.* **15**: 1069–1100. doi:10.1007/s10652-015-9407-2
- 626 Jackson, T. R., R. Haggerty, S. V. Apte, A. Coleman, and K. J. Drost. 2012. Defining and
627 measuring the mean residence time of lateral surface transient storage zones in small
628 streams. *Water Resour. Res.* **48**. doi:10.1029/2012WR012096
- 629 Jackson, T. R., R. Haggerty, S. V. Apte, and B. L. O’Connor. 2013. A mean residence time
630 relationship for lateral cavities in gravel-bed rivers and streams: Incorporating streambed
631 roughness and cavity shape. *Water Resour. Res.* **49**: 3642–3650. doi:10.1002/wrcr.20272
- 632 Kasahara, T., and S. M. Wondzell. 2003. Geomorphic controls on hyporheic exchange flow in
633 mountain streams. *Water Resour. Res.* **39**: SBH 3-1-SBH 3-14.
634 doi:10.1029/2002wr001386
- 635 Katz, S. B., C. Segura, and D. R. Warren. 2018. The influence of channel bed disturbance on
636 benthic Chlorophyll a: A high resolution perspective. *Geomorphology* **305**: 141–153.
637 doi:10.1016/j.geomorph.2017.11.010

638 Kelleher, C., T. Wagener, B. McGlynn, A. S. Ward, M. N. Gooseff, and R. A. Payn. 2013.
 639 Identifiability of transient storage model parameters along a mountain stream. *Water*
 640 *Resour. Res.* **49**: 5290–5306. doi:10.1002/wrcr.20413
 641 Kiel, B. A., and M. Bayani Cardenas. 2014. Lateral hyporheic exchange throughout the
 642 Mississippi River network. *Nat. Geosci.* **7**: 413–417. doi:10.1038/ngeo2157
 643 Knapp, J. L. A., R. González-Pinzón, J. D. Drummond, L. G. Larsen, O. A. Cirpka, and J. W.
 644 Harvey. 2017. Tracer-based characterization of hyporheic exchange and benthic biolayers
 645 in streams. *Water Resour. Res.* **53**: 1575–1594. doi:10.1002/2016WR019393
 646 Knapp, J. L. A., R. González-Pinzón, and R. Haggerty. 2018. The Resazurin-Resorufin System:
 647 Insights From a Decade of “Smart” Tracer Development for Hydrologic Applications.
 648 *Water Resour. Res.* **54**: 6877–6889. doi:10.1029/2018WR023103
 649 Knapp, J. L. A., and C. Kelleher. 2020. A Perspective on the Future of Transient Storage
 650 Modeling: Let’s Stop Chasing Our Tails. *Water Resour. Res.* **56**: e2019WR026257.
 651 doi:10.1029/2019WR026257
 652 Krause, S., J. Lewandowski, N. B. Grimm, and others. 2017. Ecohydrological interfaces as hot
 653 spots of ecosystem processes: ECOHYDROLOGICAL INTERFACES AS HOT SPOTS.
 654 *Water Resour. Res.* **53**: 6359–6376. doi:10.1002/2016WR019516
 655 Lane, C. S., D. R. Lyon, and S. E. Ziegler. 2012. Cycling of two carbon substrates of contrasting
 656 lability by heterotrophic biofilms across a nutrient gradient of headwater streams. *Aquat.*
 657 *Sci.* **75**: 235–250. doi:10.1007/s00027-012-0269-0
 658 Lautz, L. K., and D. I. Siegel. 2007. The effect of transient storage on nitrate uptake lengths in
 659 streams: an inter-site comparison. *Hydrol. Process.* **21**: 3533–3548. doi:10.1002/hyp.6569
 660 Li, L., P. L. Sullivan, P. Benettin, and others. 2021. Toward catchment hydro-biogeochemical
 661 theories. *Wiley Interdiscip. Rev. Water* **8**: 1–31. doi:10.1002/wat2.1495
 662 Li, Z., Z. Zeng, D. Tian, and others. 2020. The stoichiometry of soil microbial biomass
 663 determines metabolic quotient of nitrogen mineralization. *Environ. Res. Lett.* **15**: 034005.
 664 doi:10.1088/1748-9326/ab6a26
 665 Liu, S., T. Maavara, C. B. Brinkerhoff, and P. A. Raymond. 2022. Global Controls on DOC
 666 Reaction Versus Export in Watersheds: A Damköhler Number Analysis. *Glob.*
 667 *Biogeochem. Cycles* **36**: e2021GB007278. doi:10.1029/2021GB007278
 668 Logue, J. B., C. A. Stedmon, A. M. Kellerman, N. J. Nielsen, A. F. Andersson, H. Laudon, E. S.
 669 Lindström, and E. S. Kritzberg. 2016. Experimental insights into the importance of
 670 aquatic bacterial community composition to the degradation of dissolved organic matter.
 671 *ISME J.* **10**: 533–545. doi:10.1038/ismej.2015.131
 672 Martí, E., N. B. Grimm, and S. G. Fisher. 1997. Pre- and Post-Flood Retention Efficiency of
 673 Nitrogen in a Sonoran Desert Stream. *J. North Am. Benthol. Soc.* **16**: 805–819.
 674 doi:10.2307/1468173
 675 Mulholland, P. J., and W. R. Hill. 1997. Seasonal patterns in streamwater nutrient and dissolved
 676 organic carbon concentrations: Separating catchment flow path and in-stream effects.
 677 *Water Resour. Res.* **33**: 1297–1306. doi:10.1029/97wr00490
 678 Natural Resources Conservation Service. Web Soil Survey. U. S. Dep. Agric.
 679 Navel, S., F. Mermillod-Blondin, B. Montuelle, E. Chauvet, L. Simon, and P. Marmonier. 2011.
 680 Water-Sediment Exchanges Control Microbial Processes Associated with Leaf Litter
 681 Degradation in the Hyporheic Zone: A Microcosm Study. *Microb. Ecol.* **61**: 968–979.
 682 doi:10.1007/s00248-010-9774-7

- 683 Niyogi, D. K., K. S. Simon, and C. R. Townsend. 2004. Land use and stream ecosystem
684 functioning: nutrient uptake in streams that contrast in agricultural development. *Arch.*
685 *Für Hydrobiol.* **160**: 471–486. doi:10.1127/0003-9136/2004/0160-0471
- 686 Ocampo, C., Oldham, C., and Sivapalan, M. 2020. Nitrate attenuation in agricultural catchments:
687 Shifting balances between transport and reaction - Ocampo - 2006 - *Water Resources*
688 *Research - Wiley Online Library.*
- 689 Oldham, C. E., D. E. Farrow, and S. Peiffer. 2013. A generalized Damköhler number for
690 classifying material processing in hydrological systems. *Hydrol. Earth Syst. Sci.* **17**:
691 1133–1148. doi:10.5194/hess-17-1133-2013
- 692 Perkins, D. M., G. Yvon-Durocher, B. O. L. Demars, J. Reiss, D. E. Pichler, N. Friberg, M.
693 Trimmer, and G. Woodward. 2012. Consistent temperature dependence of respiration
694 across ecosystems contrasting in thermal history. *Glob. Change Biol.* **18**: 1300–1311.
695 doi:10.1111/j.1365-2486.2011.02597.x
- 696 Pinay, G., S. Peiffer, J.-R. De Dreuzy, and others. 2015. Upscaling Nitrogen Removal Capacity
697 from Local Hotspots to Low Stream Orders' Drainage Basins. *Ecosystems* **18**: 1101–
698 1120. doi:10.1007/s10021-015-9878-5
- 699 Ries III, K. G., J. K. Newson, M. J. Smith, and others. 2017. StreamStats, version 4.
- 700 Rodríguez-Cardona, B., A. S. Wymore, and W. H. McDowell. 2016. DOC:NO₃⁻ ratios and
701 NO₃⁻ uptake in forested headwater streams. *J. Geophys. Res. Biogeosciences* **121**: 205–
702 217. doi:10.1002/2015JG003146
- 703 Ryan, R. J., A. I. Packman, and S. S. Kilham. 2007. Relating phosphorus uptake to changes in
704 transient storage and streambed sediment characteristics in headwater tributaries of
705 Valley Creek, an urbanizing watershed. *J. Hydrol.* **336**: 444–457.
706 doi:10.1016/j.jhydrol.2007.01.021
- 707 Schmid, B. H., I. Innocenti, and U. Sanfilippo. 2010. Characterizing solute transport with
708 transient storage across a range of flow rates: The evidence of repeated tracer
709 experiments in Austrian and Italian streams. *Adv. Water Resour.* **33**: 1340–1346.
710 doi:10.1016/j.advwatres.2010.06.001
- 711 Sheibley, R. W., J. H. Duff, and A. J. Tesoriero. 2014. Low Transient Storage and Uptake
712 Efficiencies in Seven Agricultural Streams: Implications for Nutrient Demand. *J.*
713 *Environ. Qual.* **43**: 1980–1990. doi:10.2134/jeq2014.01.0034
- 714 Smith, R. A., R. B. Alexander, and G. E. Schwarz. 2003. Natural background concentrations of
715 nutrients in streams and rivers of the conterminous United States. *Environ. Sci. Technol.*
716 **37**: 3039–3047. doi:10.1021/es020663b
- 717 Thomas, S. A., H. Maurice Valett, J. R. Webster, and P. J. Mulholland. 2003. A regression
718 approach to estimating reactive solute uptake in advective and transient storage zones of
719 stream ecosystems. *Adv. Water Resour.* **26**: 965–976. doi:10.1016/S0309-
720 1708(03)00083-6
- 721 Trentman, M. T., W. K. Dodds, J. S. Fencl, K. Gerber, J. Guarneri, S. M. Hitchman, Z. Peterson,
722 and J. Rüegg. 2015. Quantifying ambient nitrogen uptake and functional relationships of
723 uptake versus concentration in streams: a comparison of stable isotope, pulse, and plateau
724 approaches. *Biogeochemistry* **125**: 65–79.
- 725 Tromboni, F., S. A. Thomas, B. Gücker, and others. 2018. Nutrient Limitation and the
726 Stoichiometry of Nutrient Uptake in a Tropical Rain Forest Stream. *J. Geophys. Res.*
727 *Biogeosciences* **123**: 2154–2167. doi:10.1029/2018JG004538

- 728 Valett, H. M., J. A. Morrice, C. N. Dahm, and M. E. Campana. 1996. Parent lithology, surface-
729 groundwater exchange, and nitrate retention in headwater streams. *Limnol. Oceanogr.* **41**:
730 333–345. doi:10.4319/lo.1996.41.2.0333
- 731 Vrugt, J. A., C. J. F. Ter Braak, C. G. H. Diks, B. A. Robinson, J. M. Hyman, and D. Higdon.
732 2009. Accelerating Markov Chain Monte Carlo Simulation by Differential Evolution
733 with Self-Adaptive Randomized Subspace Sampling. *Int. J. Nonlinear Sci. Numer. Simul.*
734 **10**. doi:10.1515/IJNSNS.2009.10.3.273
- 735 Wagner, K., M. M. Bengtsson, R. H. Findlay, T. J. Battin, and A. J. Ulseth. 2017. High light
736 intensity mediates a shift from allochthonous to autochthonous carbon use in
737 phototrophic stream biofilms. *J. Geophys. Res. Biogeosciences* **122**: 1806–1820.
738 doi:10.1002/2016JG003727
- 739 Ward, A. S., and A. I. Packman. 2019. Advancing our predictive understanding of river corridor
740 exchange. *Wiley Interdiscip. Rev. Water* **6**: e1327. doi:10.1002/wat2.1327
- 741 Ward, A. S., R. A. Payn, M. N. Gooseff, B. L. McGlynn, K. E. Bencala, C. A. Kelleher, S. M.
742 Wondzell, and T. Wagener. 2013. Variations in surface water-ground water interactions
743 along a headwater mountain stream: Comparisons between transient storage and water
744 balance analyses. *Water Resour. Res.* **49**: 3359–3374. doi:10.1002/wrcr.20148
- 745 Webster, J. R., P. J. Mulholland, J. L. Tank, and others. 2003. Factors affecting ammonium
746 uptake in streams - an inter-biome perspective. *Freshw. Biol.* **48**: 1329–1352.
747 doi:10.1046/j.1365-2427.2003.01094.x
- 748 Wen, H., and L. Li. 2018. An upscaled rate law for mineral dissolution in heterogeneous media:
749 The role of time and length scales. *Geochim. Cosmochim. Acta* **235**: 1–20.
750 doi:10.1016/j.gca.2018.04.024
- 751 Wilhelm, L., K. Besemer, L. Fragner, H. Peter, W. Weckwerth, and T. J. Battin. 2015.
752 Altitudinal patterns of diversity and functional traits of metabolically active
753 microorganisms in stream biofilms. *ISME J.* **9**: 2454–2464. doi:10.1038/ismej.2015.56
- 754 Wondzell, S. M. 2006. Effect of morphology and discharge on hyporheic exchange flows in two
755 small streams in the Cascade Mountains of Oregon, USA. *Hydrol. Process.* **20**: 267–287.
756 doi:10.1002/hyp.5902
- 757 Zarnetske, J. P., M. N. Gooseff, T. R. Brosten, J. H. Bradford, J. P. McNamara, and W. B.
758 Bowden. 2007. Transient storage as a function of geomorphology, discharge, and
759 permafrost active layer conditions in Arctic tundra streams. *Water Resour. Res.* **43**: 7410.
760 doi:10.1029/2005WR004816
- 761 Zarnetske, J. P., R. Haggerty, S. M. Wondzell, V. A. Bokil, and R. González-Pinzón. 2012.
762 Coupled transport and reaction kinetics control the nitrate source-sink function of
763 hyporheic zones. *Water Resour. Res.* **48**. doi:10.1029/2012wr011894
764